Electronic Supplementary Material (ESI) for CrystEngComm.

Hierarchical importance of coordination and hydrogen bonds in the formation of homochiral 2D coordination polymers and 2D supramolecular assemblies

Navnita Kumar, Sadhika Khullar and Sanjay K. Mandal*

Department of Chemical Sciences, Indian Institute of Science Education and Research, Mohali, Sector 81, Manauli PO, S.A.S. Nagar, Mohali (Punjab) 140306, INDIA

Supplementary Information

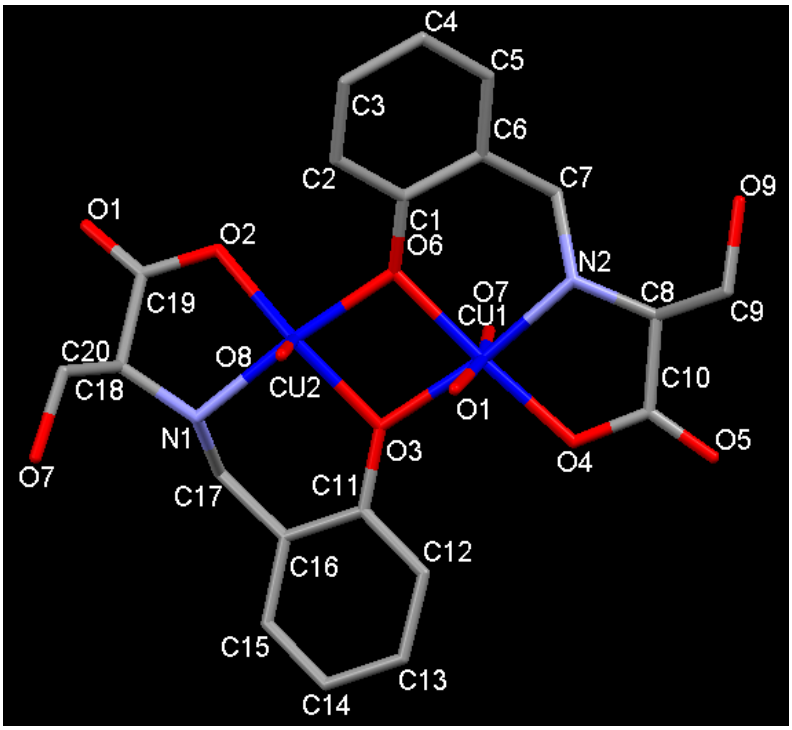

Fig. S1 Dinuclear subunit in **1**. Hydrogen atoms are omitted for clarity.

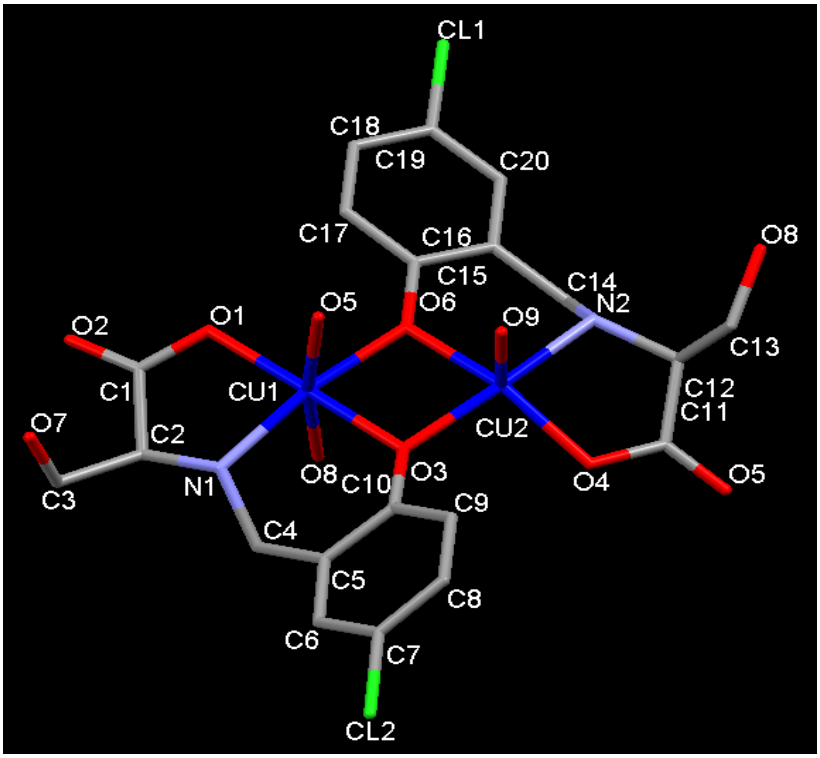

Fig. S2 Dinuclear subunit in **4**. Hydrogen atoms are omitted for clarity.

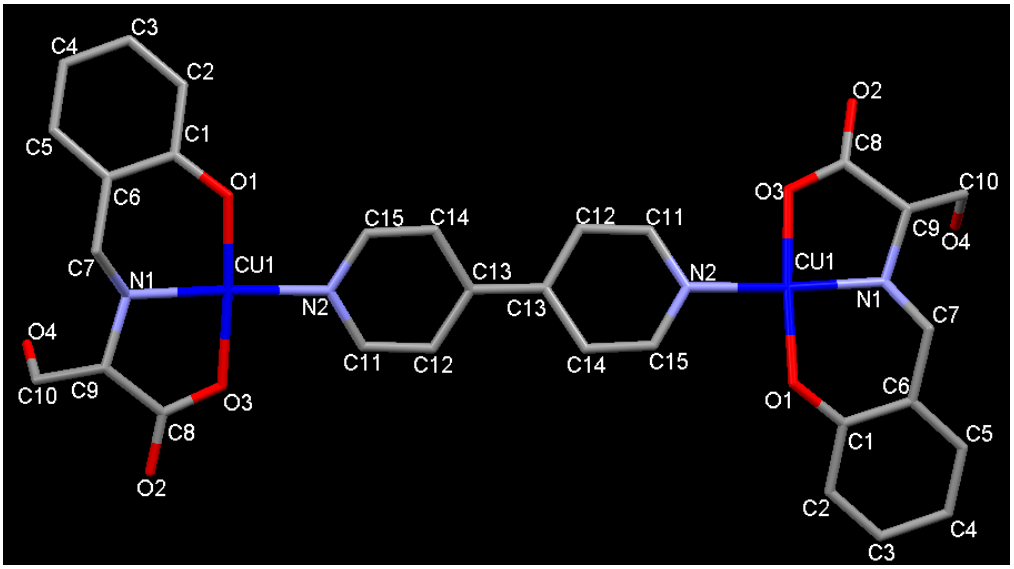

Fig. S3. Dinuclear subunit in **7**. Hydrogen atoms are omitted for clarity.

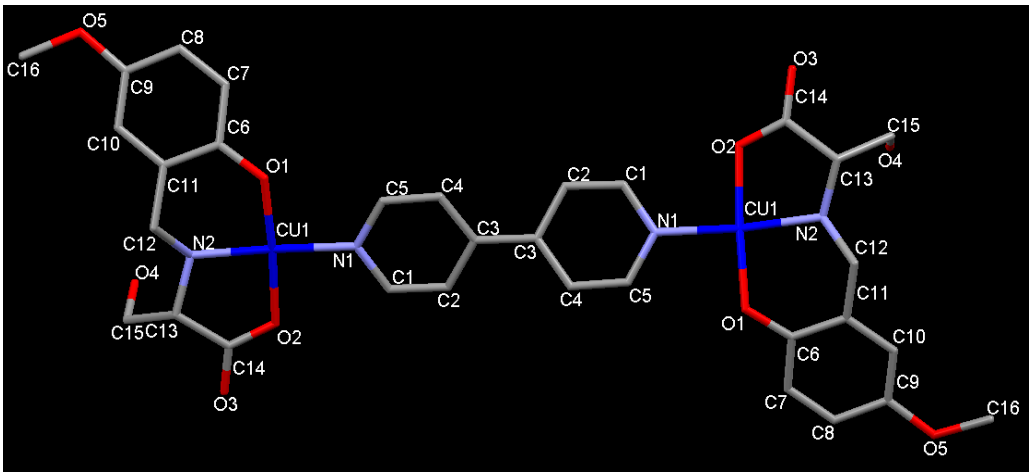

Fig. S4. Dinuclear subunit in **8**. Hydrogen atoms are omitted for clarity.

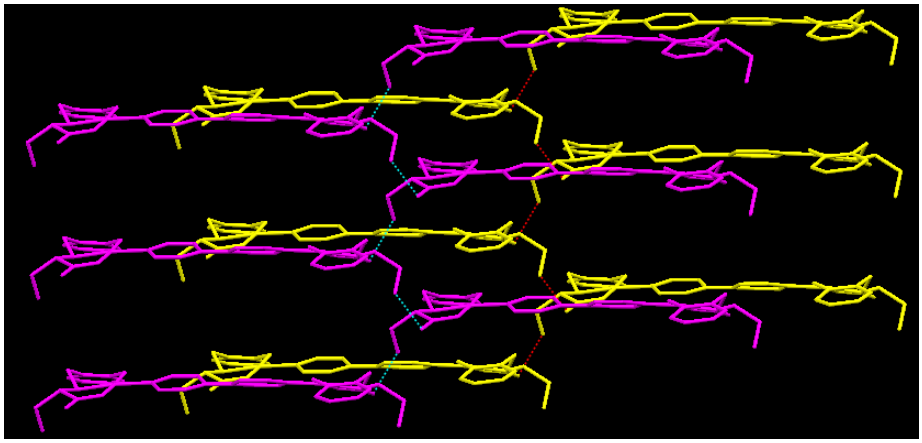

Fig. S5 Two layers of discrete unit (one layer shown in magenta other in yellow) each forming 2D supramolecular assembly via hydrogen bonding (for one layer shown in green other shown in red) in **7**.

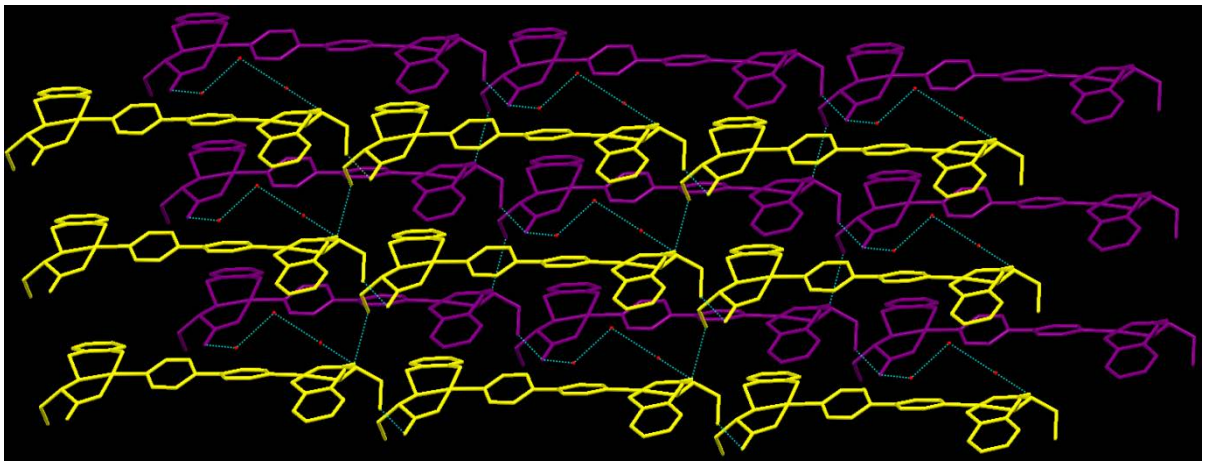

Fig. S6a Two 2D supramolecular assembly joined via solvent molecules in **7**. Hydrogen atoms are omitted for clarity

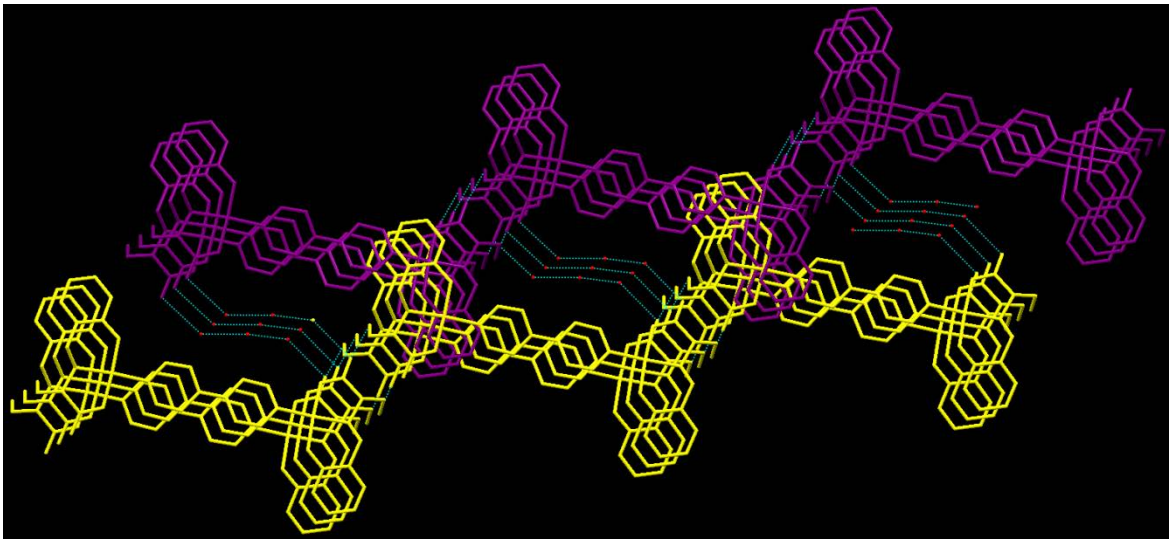

Fig. S6b Another view of solvent molecules joining the two 2D supramolecular assemblies in **7**.

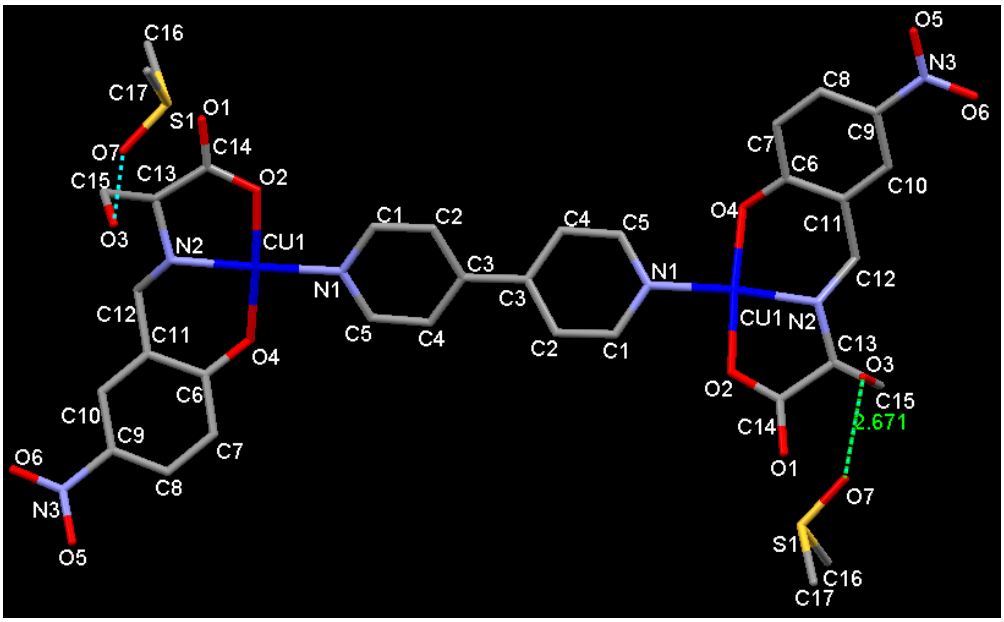

Fig. S7 Dinuclear unit in **9**. Also shown hydrogen bonding with the lattice DMSO molecules. Hydrogen atoms are omitted for clarity

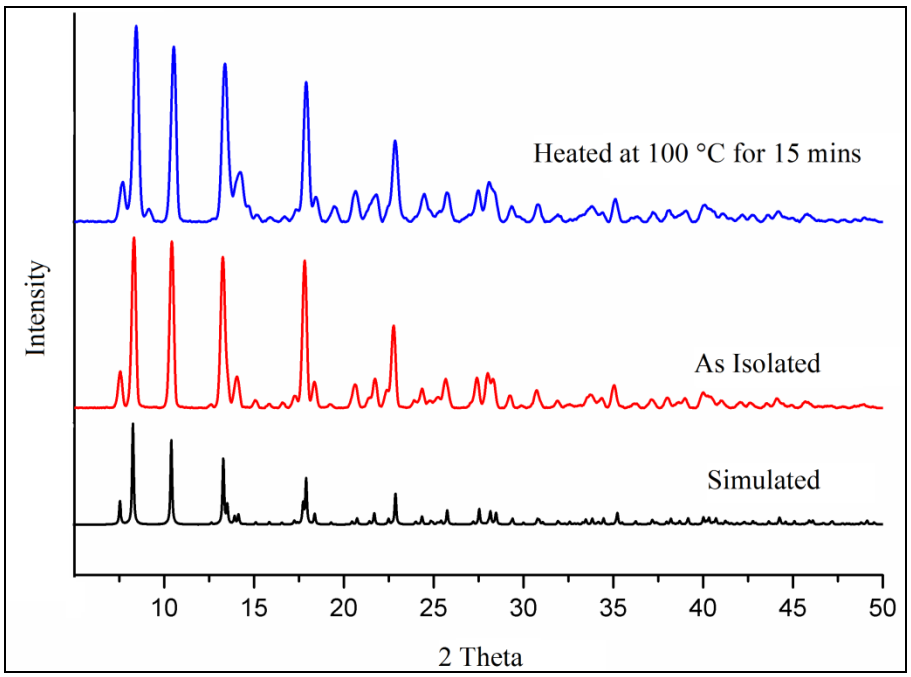

Fig. S8 Experimental and simulated X-ray powder patterns for **1.**

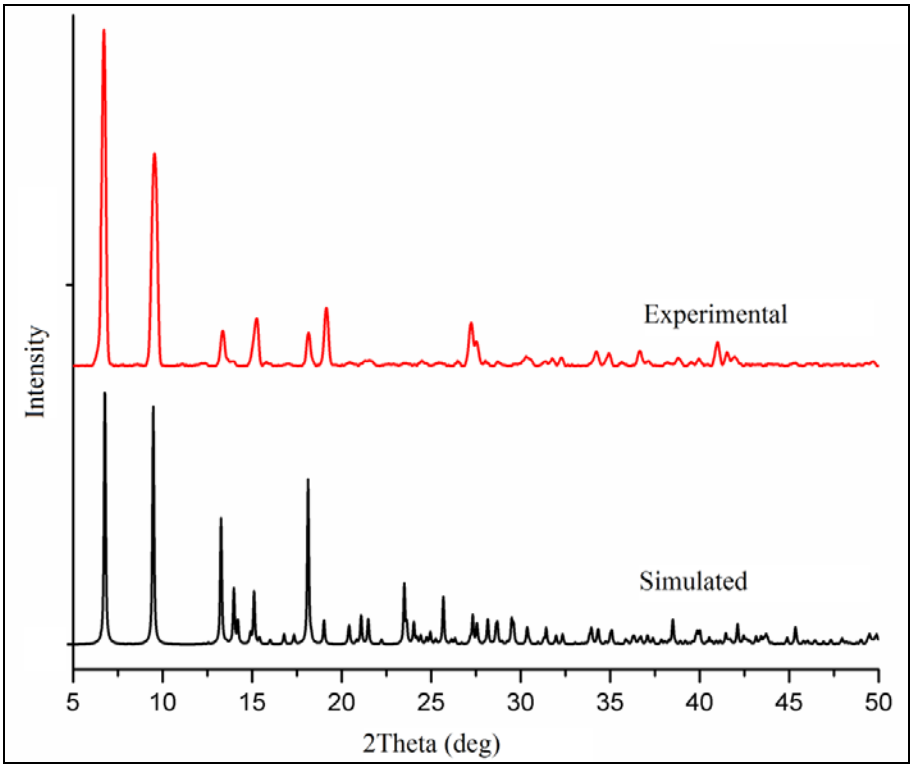

Fig. S9 Experimental and simulated X-ray powder patterns for **4**.

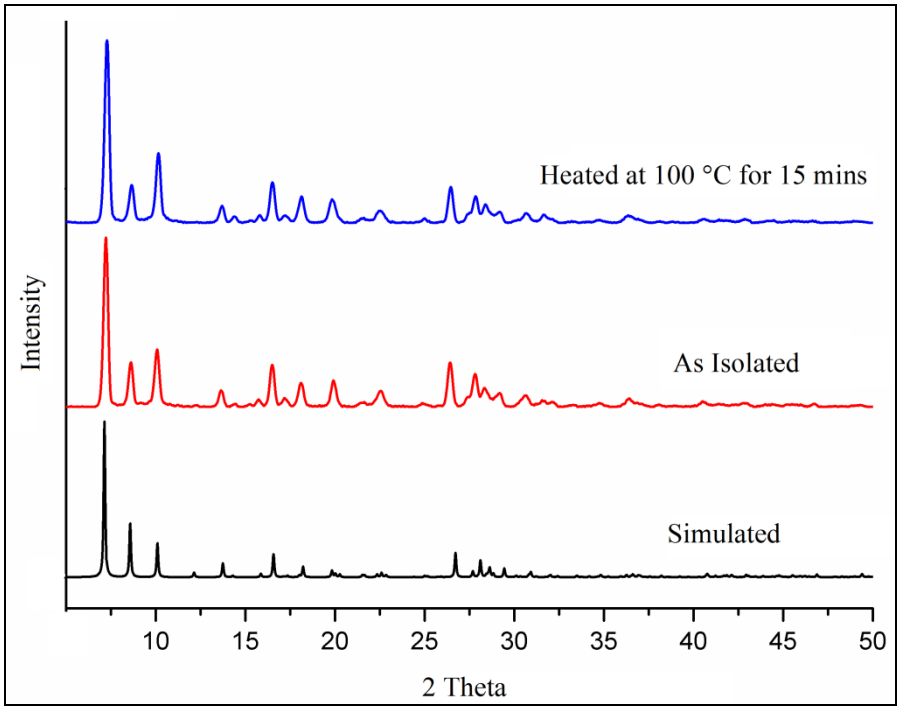

Fig. S10 Experimental and simulated X-ray powder patterns for **7**.

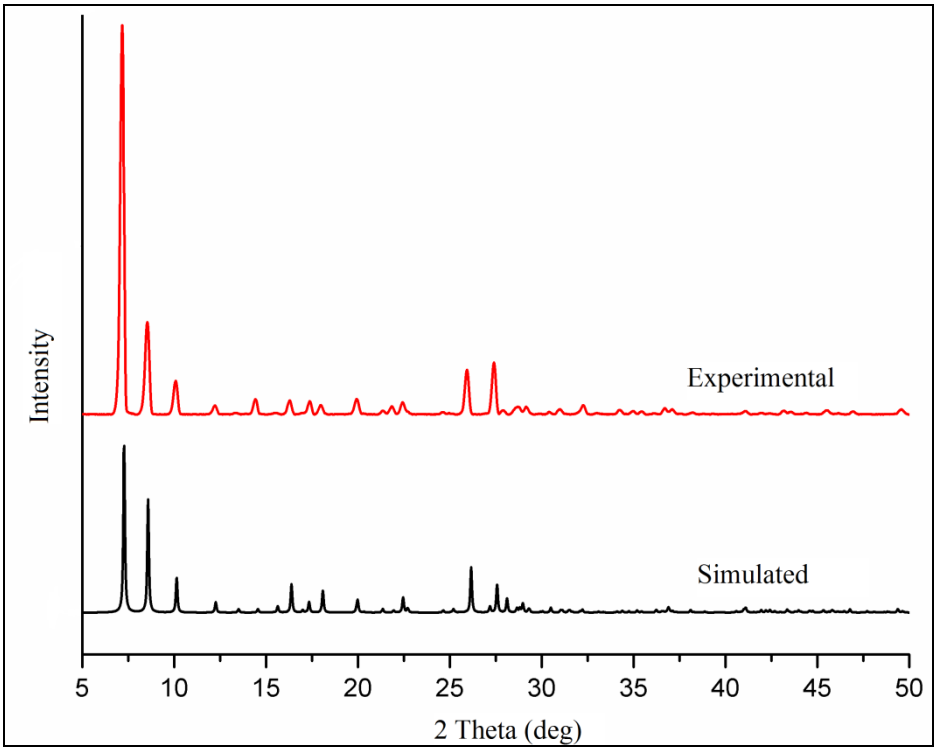

Fig. S11 Experimental and simulated X-ray powder patterns for **8**.

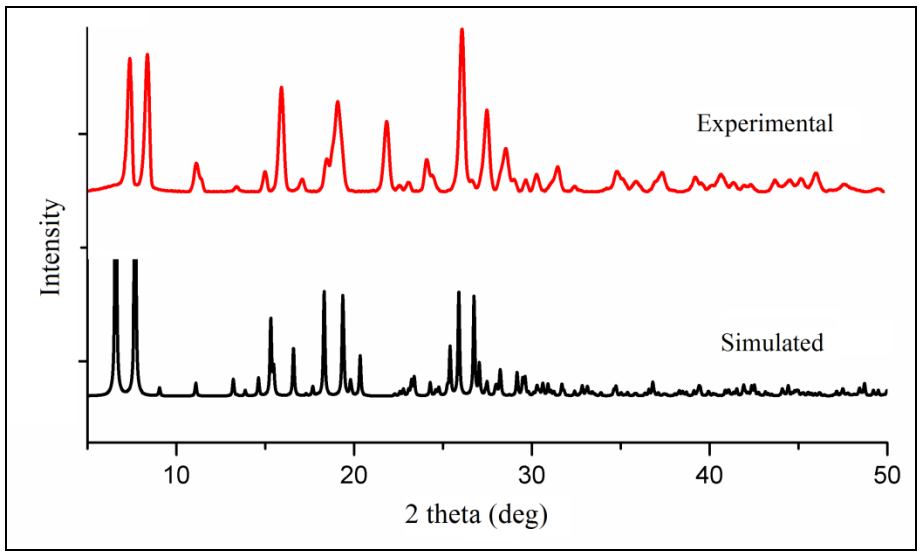

Fig. S12 Experimental and simulated X-ray powder patterns for **9**.

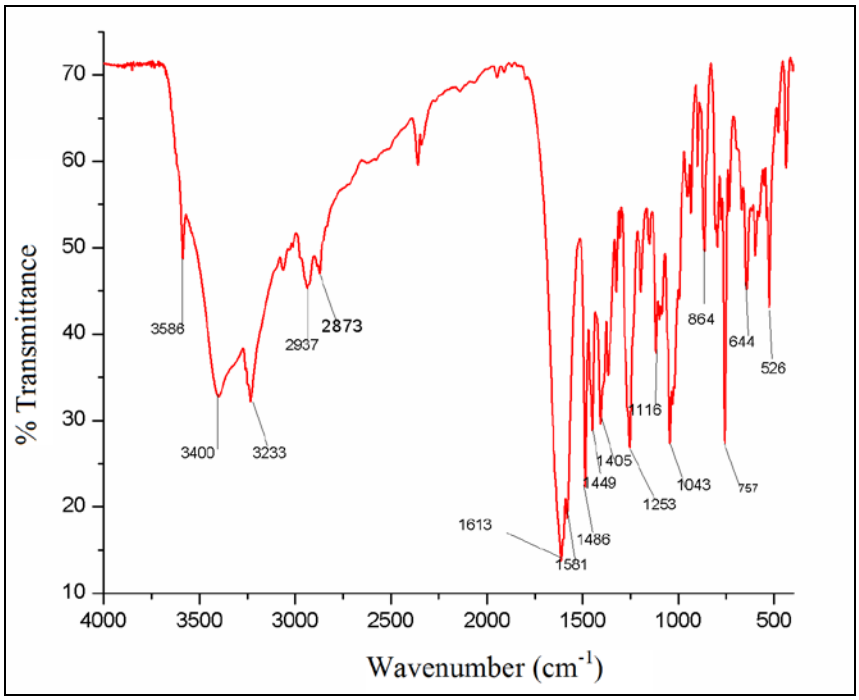

Fig. S13 FTIR Spectrum for **1**.

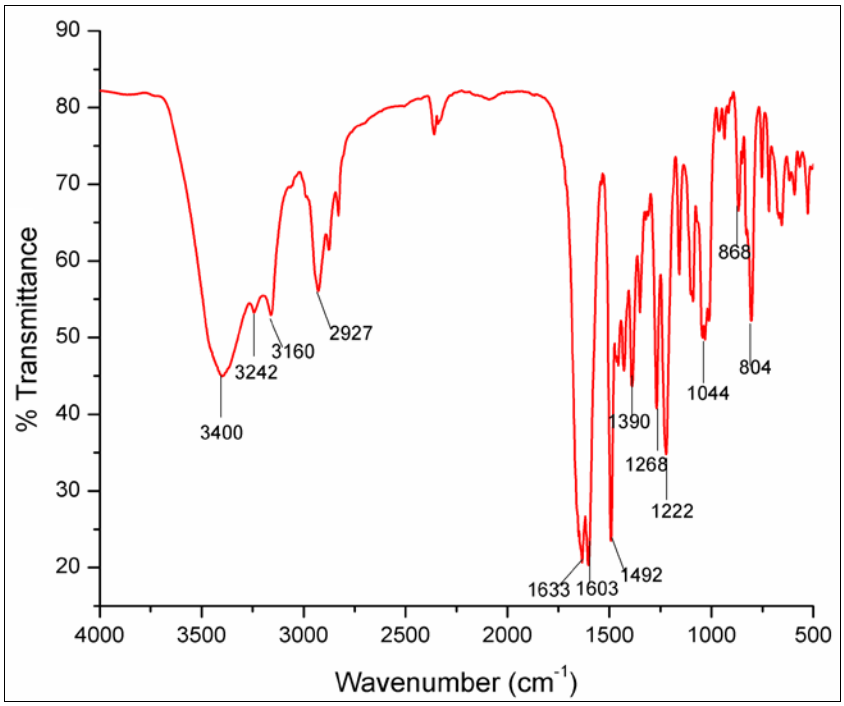

Fig. S14 FTIR spectrum for **2**.

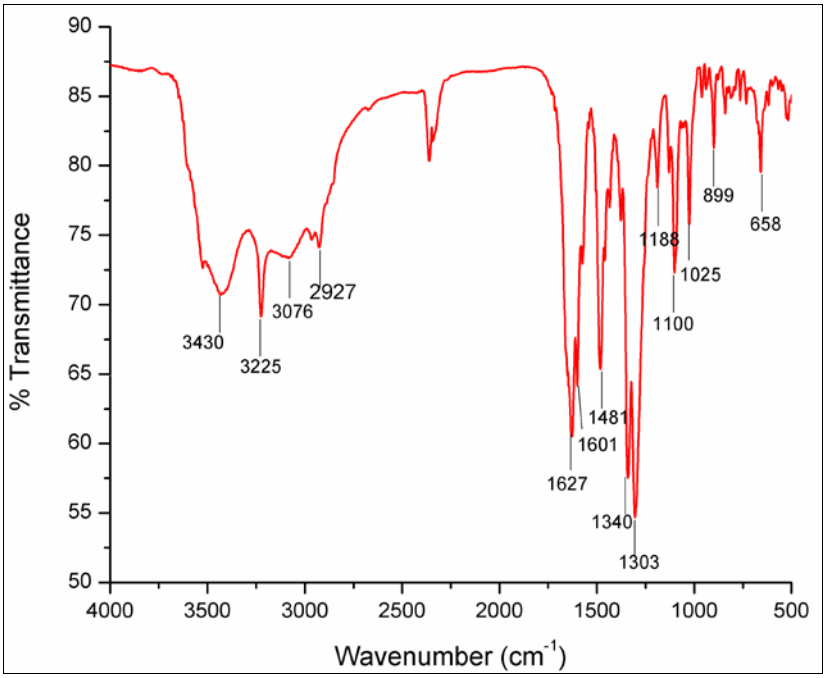

Fig. S15 FTIR spectrum for **3**.

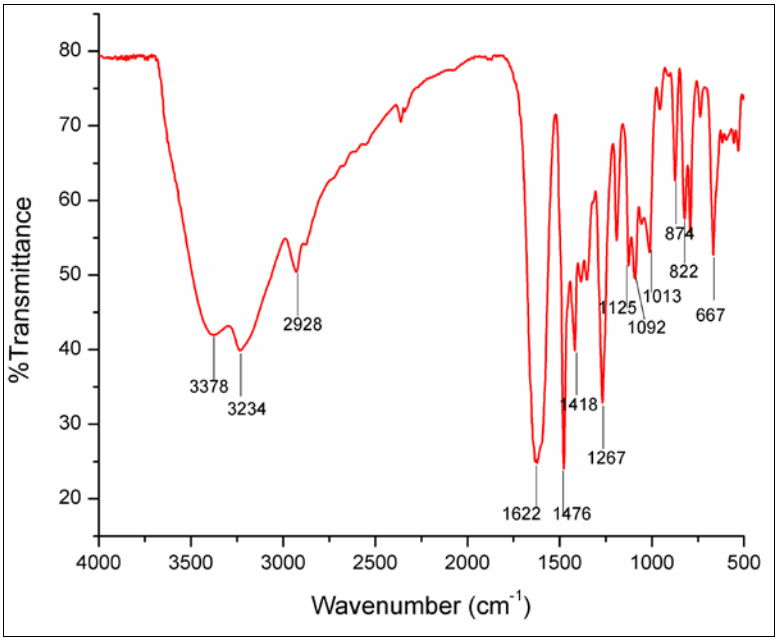

Fig. S16 FTIR spectrum for **4**.

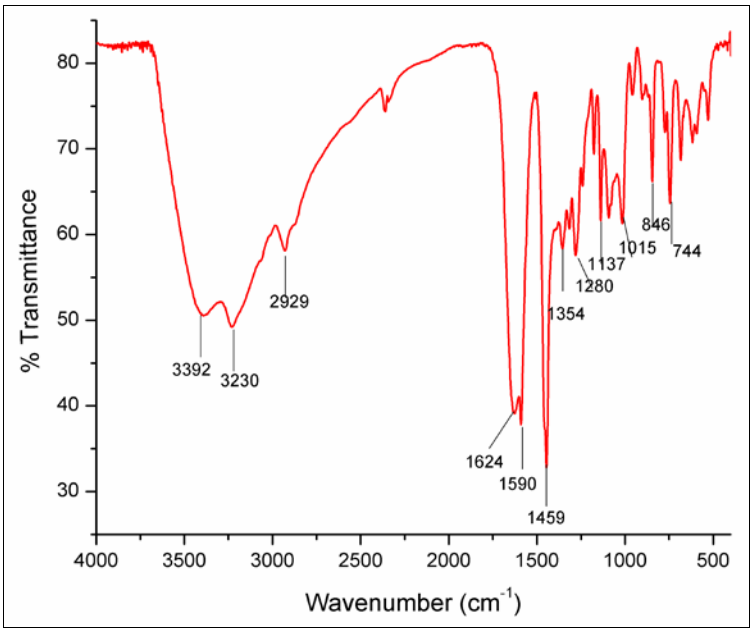

Fig. S17 FTIR spectrum for **5.**

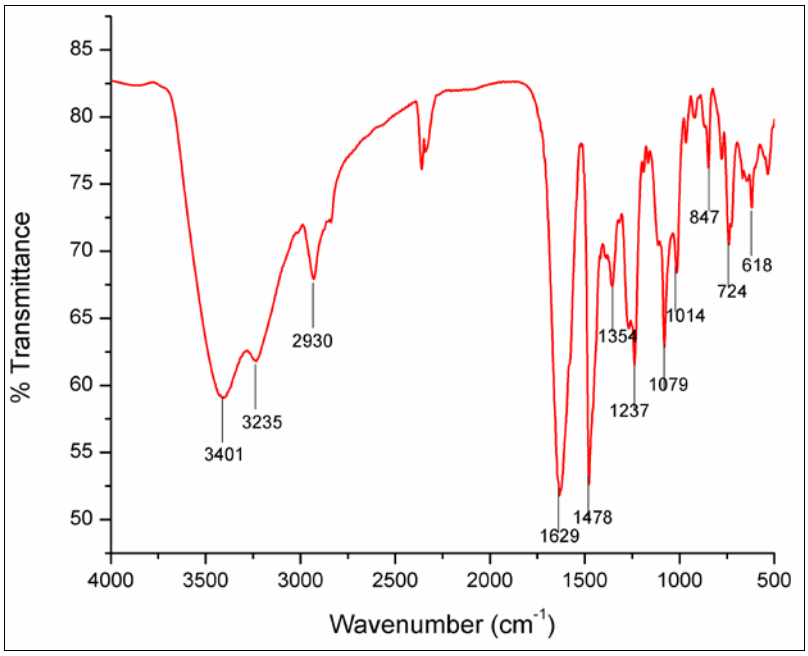

Fig. S18 FTIR spectrum for **6.**

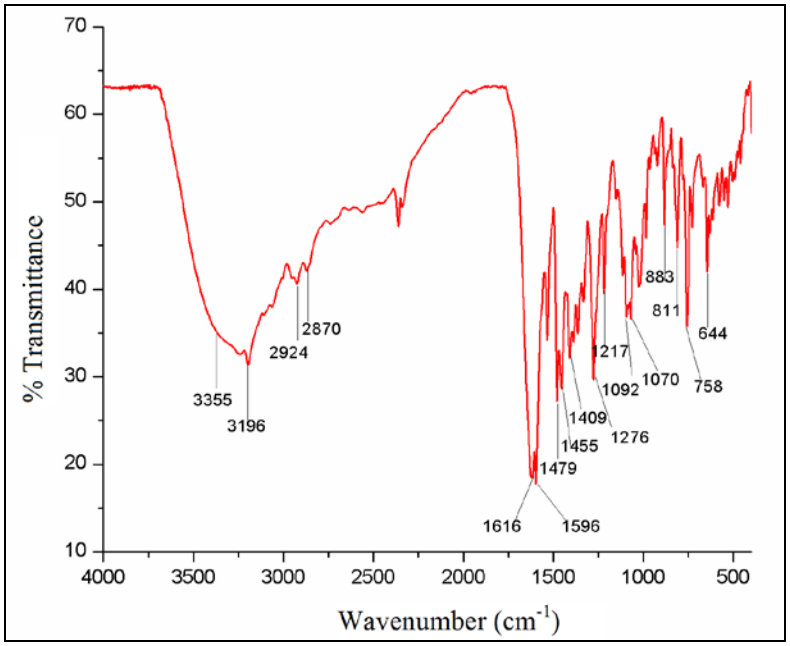

Fig. S19 FTIR spectrum for **7**.

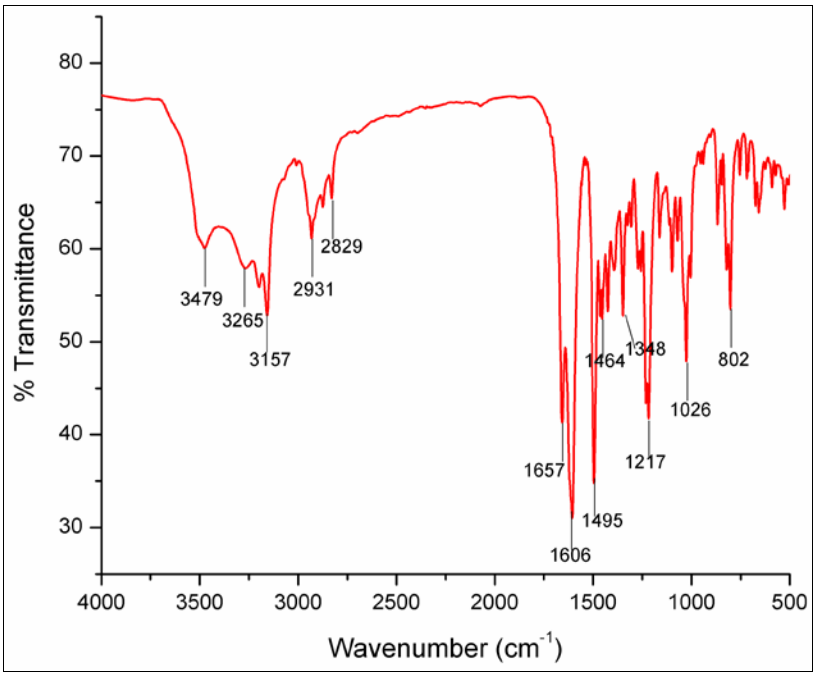

Fig. S20 FTIR spectrum for **8**.

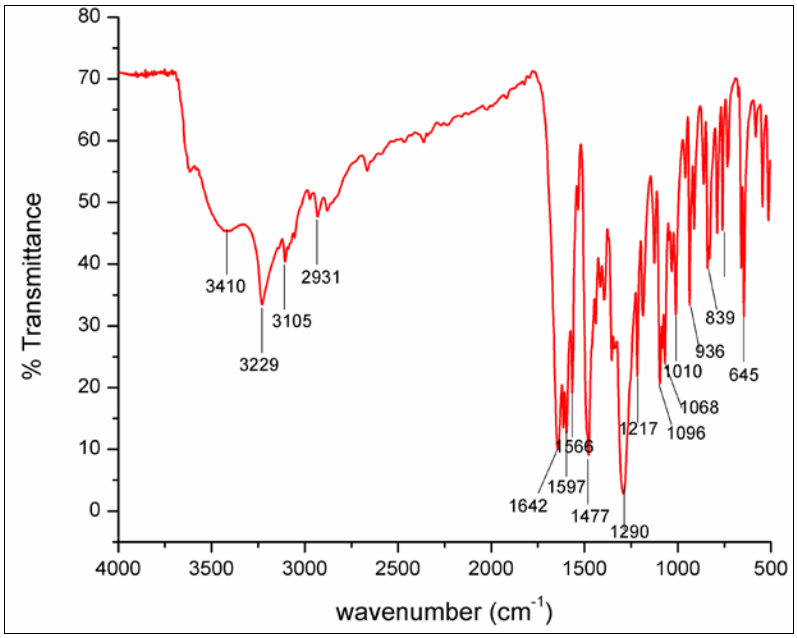

Fig. S21 FTIR spectrum for **9**.

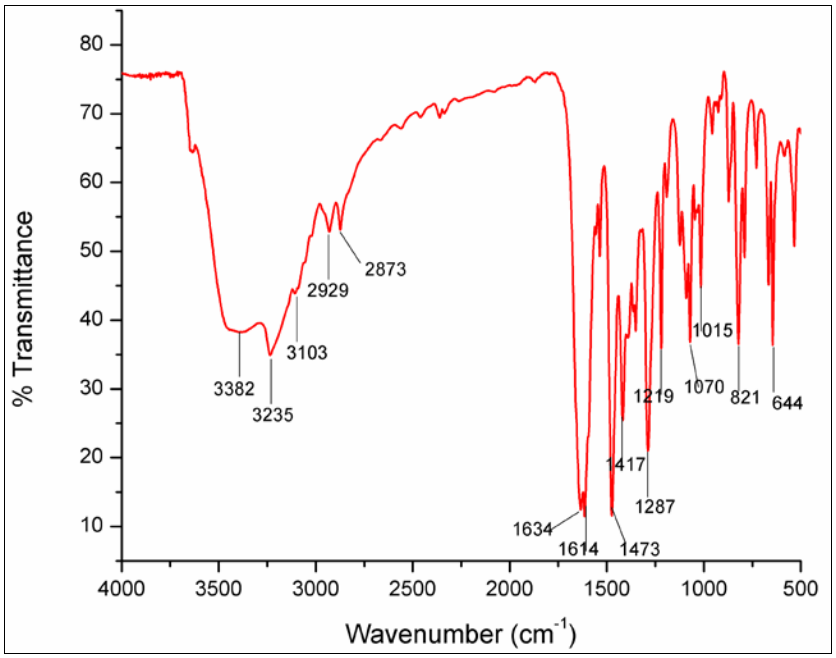

Fig. S22 FTIR spectrum for **10**.

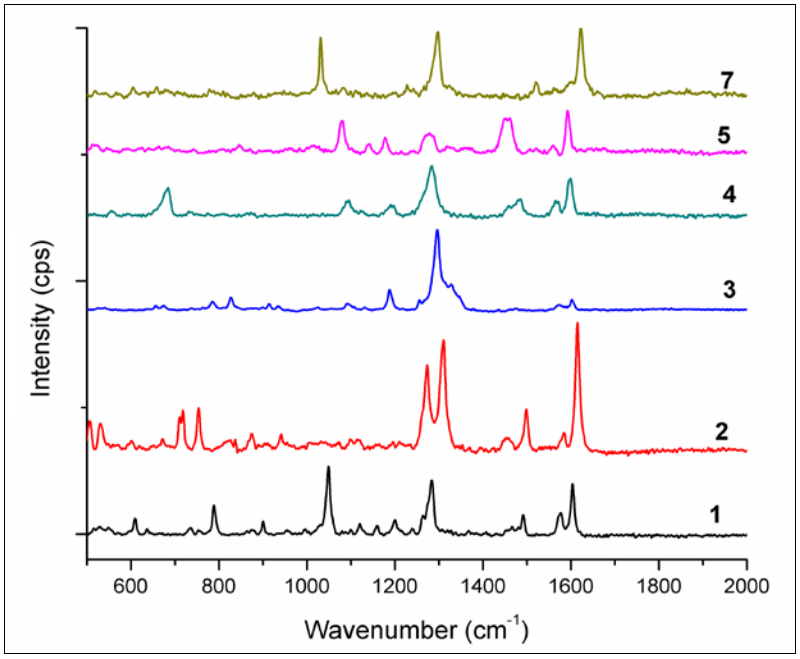

Fig. S23 Raman spectra of **1, 2, 3, 4, 5** and **7**.

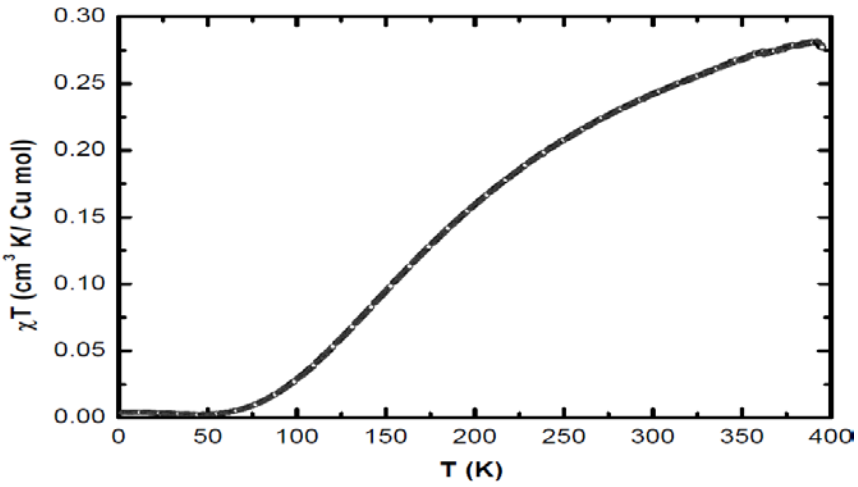

Fig. S23 Plot of χT versus T data for **1**.

Table S1. Selected Bond lengths (Å) for **1**, **4**, **7**, **8** and **9**.

1			
Cu2-O6	1.920(5)	Cu2-O2	1.950(4)
Cu2-O3	1.973(5)	Cu2-N1	1.982(6)
Cu2-O8	2.360(5)	Cu1-O4	1.950(5)
Cu1-O6	1.958(5)	Cu1-N2	1.983(6)
Cu1-O3	1.989(5)	Cu1-O7	2.389(5)
4			
Cu1-O3	1.925(2)	Cu1-O1	1.925(2)
Cu1-N1	1.966(3)	Cu1-O6	1.971(2)
Cu2-O9	2.257(3)	Cu2-O3	1.931(2)
Cu2-O4	1.939(2)	Cu2-O6	1.964(2)
Cu2-N2	1.984(3)		
7			
Cu1-O1	1.909(6)	Cu1-O3	1.933(6)
Cu1-N1	1.984(7)	Cu1-N2	1.997(7)
8			
Cu1-O1	1.898(4)	Cu1-O2	1.952(5)
Cu1-N2	1.979(6)	Cu1-N1	1.997(5)
9			
Cu1-O2	1.906(6)	Cu1-O4	1.930(6)
Cu1-N2	1.981(8)	Cu1-N1	1.991(7)

Table S2. Selected Bond angles (degrees) for **1**, **4**, **7**, **8** and **9**.

1			
O6-Cu2-O2	98.2(2)	O6-Cu2-O3	80.1(2)
O2-Cu2-O3	151.5(2)	O6-Cu2-N1	174.1(2)
O2-Cu2-N1	86.0(2)	O3-Cu2-N1	94.3(2)
O6-Cu2-O8	90.8(2)	O2-Cu2-O8	109.5(2)
O3-Cu2-O8	99.06(19)	N1-Cu2-O8	91.8(2)
O4-Cu1-O6	176.7(2)	O4-Cu1-N2	84.3(2)
O6-Cu1-N2	93.4(2)	O4-Cu1-O3	103.5(2)
O6-Cu1-O3	78.8(2)	N2-Cu1-O3	172.1(2)
O4-Cu1-O7	91.52(18)	O6-Cu1-O7	86.31(19)
N2-Cu1-O7	96.4(2)	O3-Cu1-O7	84.21(19)
Cu2-O8-H8A	110.1	Cu2-O8-H8B	109.5
C18-N1-Cu2	108.5(4)	C17-N1-Cu2	107.6(4)
C11-O3-Cu2	124.1(4)	C11-O3-Cu1	135.3(4)

Cu2-O3-Cu1	98.6(2)	C10-O4-Cu1	115.4(4)
C1-O6-Cu2	128.1(4)	C1-O6-Cu1	124.4(4)
Cu2-O6-Cu1	101.5(2)	C20-O7-Cu1	115.6(4)
Cu2-N1-H1	108.9	Cu1-O7-H7	125.(2)
C19-O2-Cu2	114.4(4)	Cu1-N2-H2	107.5
C8-N2-Cu1	109.5(4)	C7-N2-Cu1	110.5(4)

4

O3-Cu1-O1	177.01(11)	O3-Cu1-N1	93.95(10)
O1-Cu1-N1	84.64(10)	O3-Cu1-O6	79.19(9)
O1-Cu1-O6	102.57(10)	N1-Cu1-O6	169.42(10)
O3-Cu1-Cu2	39.07(7)	O1-Cu1-Cu2	142.43(7)
N1-Cu1-Cu2	132.93(8)	O6-Cu1-Cu2	40.30(7)
O3-Cu2-O4	97.39(10)	O3-Cu2-O6	79.21(10)
O4-Cu2-O6	154.69(11)	O3-Cu2-N2	169.36(11)
O4-Cu2-N2	85.70(10)	O6-Cu2-N2	93.62(10)
O3-Cu2-O9	91.35(10)	O4-Cu2-O9	104.62(10)
O6-Cu2-O9	100.54(10)	N2-Cu2-O9	97.73(11)
O3-Cu2-Cu1	38.91(7)	O4-Cu2-Cu1	133.05(7)
O6-Cu2-Cu1	40.48(7)	N2-Cu2-Cu1	134.02(8)
O9-Cu2-Cu1	94.70(7)	C1-O1-Cu1	114.7(2)
C10-O3-Cu1	123.5(2)	C10-O3-Cu2	132.1(2)
Cu1-O3-Cu2	102.02(11)	C11-O4-Cu2	115.4(2)
C2-N1-C4	114.1(3)	C2-N1-Cu1	107.7(2)
C4-N1-Cu1	111.0(2)	C2-N1-H1	108
C4-N1-H1	108	Cu1-N1-H1	108
C16-O6-Cu2	126.3(2)	C16-O6-Cu1	134.4(2)
Cu2-O6-Cu1	99.22(11)	Cu2-N2-H11A	108.5
C12-N2-Cu2	109.0(2)	C14-N2-Cu2	108.1(2)

7

O1-Cu1-O3	176.2(3)	O1-Cu1-N1	92.7(3)
O3-Cu1-N1	83.7(3)	O1-Cu1-N2	92.0(3)
O3-Cu1-N2	91.7(3)	N1-Cu1-N2	172.4(4)
C8-O3-Cu1	117.7(6)	C1-O1-Cu1	124.9(5)
C15-N2-Cu1	120.9(6)	C7-N1-Cu1	112.9(5)
C9-N1-Cu1	109.6(5)	C11-N2-Cu1	122.4(6)
Cu1-N1-H1	107.2		

8

O1-Cu1-O2	176.3(2)	O1-Cu1-N2	93.7(2)
O2-Cu1-N2	83.1(2)	O1-Cu1-N1	91.44(19)
O2-Cu1-N1	91.9(2)	N2-Cu1-N1	173.2(4)
Cu1-N2-H4	106.3	C1-N1-Cu1	121.4(4)

C5-N1-Cu1	121.5(4)	C13-O2-Cu1	116.2(5)
C12-N2-Cu1	110.3(4)	C11-N2-Cu1	113.0(5)
C6-O1-Cu1	123.2(4)		

9

O2-Cu1-O4	172.6(3)	O2-Cu1-N2	83.8(3)
O4-Cu1-N2	93.9(3)	O2-Cu1-N1	91.1(3)
O4-Cu1-N1	92.1(3)	N2-Cu1-N1	170.2(4)
Cu1-N2-H2	106.5	C5-N1-Cu1	122.2(6)
C1-N1-Cu1	120.9(6)	O5-N3-C9	118.5(8)
C12-N2-Cu1	113.1(6)	C13-N2-Cu1	109.6(5)
C14-O2-Cu1	116.9(6)	C6-O4-Cu1	122.0(5)

Table S3. FTIR stretching frequencies for **1-6.**

Compound	ν_{OH} (cm^{-1})	ν_{NH} (cm^{-1})	$\nu_{(COO^-, asymm)}$ (cm^{-1})	$\nu_{(COO^-, symm)}$ (cm^{-1})	$\nu_{C\text{-}O\ (phenoxo)}$ (cm^{-1})
1	3400	3233	1613, 1581	1486, 1363	1276
2	3389	3242	1633, 1603	1492, 1390	1268
3	3430	3225	1627, 1601	1481, 1344	1303
4	3378	3234	1622 (br), 1594	1476, 1352	1267
5	3392	3230	1627, 1590	1458, 1394	1280
6	3401	3235	1629, 1576	1478, 1354	1267

Table S4. FTIR stretching frequencies for 7**-10.**

Compound	ν_{OH} (cm^{-1})	ν_{NH} (cm^{-1})	$\nu_{(COO^-, asymm)}$ (cm^{-1})	$\nu_{(COO^-, symm)}$ (cm^{-1})	$\nu_{C\text{-}O\ (phenoxo)}$ (cm^{-1})	from 4,4′-bipyridine (cm^{-1})
7	3355	3196	1616	1479	1276	1217
8	3479	3265	1657	1495	1272	1217
9	3410	3229	1642	1477	1290	1217
10	3382	3235	1634	1473	1287	1219

Table S5. UV-vis data for **1-6** (350 nm – 700 nm).

Compound	λ, nm (ε, $L \cdot mol^{-1} \cdot cm^{-1}$)	λ, nm (ε, $L \cdot mol^{-1} \cdot cm^{-1}$)
1	675 (123)	371 (883)
2	680 (48)	400 (296)
3	684 (70)	372 (2257)
4	663 (34)	379 (328)
5	679 (64)	376 (331)
6	672 (55)	418 (519)

Table S6. UV-vis data for **7-10** (350 nm – 700 nm).

Compound	λ, nm (ε, $L \cdot mol^{-1} \cdot cm^{-1}$)	λ, nm (ε, $L \cdot mol^{-1} \cdot cm^{-1}$)
7	655 (213)	389 (736)
8	657 (40)	394 (289)
9	680 (40)	392 (4757)
10	673 (21)	403 (137)

Table S7. Peaks in CD spectra of **1-6.**

Compound	Positive Cotton Effect (nm)	Negative Cotton Effect (nm)
1	650, 495, 265, 245, 208	600, 400, 309, 225, 222
2	654, 265, 245	565, 435, 299, 262, 224
3	664, 345, 236, 212	403, 306, 221
4	644, 273, 273, 251	482, 401, 295, 221
5	651, 504, 271, 245	575, 394, 296, 223
6	664, 524, 267, 247	569, 416, 225

Table S8. Peaks in CD spectra of **7-10.**

Compound	Positive Cotton Effect (nm)	Negative Cotton Effect (nm)
7	630, 260, 240, 200	500, 400, 309
8	648, 340, 271, 245	512, 430, 309
9	641, 343, 292	537, 399, 305, 264
10	658, 277, 251	487, 396, 308

Table S9. Thermogravimetric analysis for **1-6**.

Compound	1st step loss			2nd Step loss		
	Obsd. %	Calcd. %	Loss	Obsd. %	Calcd. %	Loss
1	9.30	10.30	2.5 H_2O (l), H_2O (c)	58.60	57.98	Ligands (H_3Sersal+serine)
2	11.67	10.50	DMF (l)	45.67	48.49	H_2O (c), Metal-ligand complex
3	6.33	5.22	2 H_2O (l)	79.53	76.52	H_2O (c), Ligand
4	5.38	5.53	H_2O (l)	49.02	46.60	H_2O (c), Metal-ligand complex
5	10.22	10.49	3 H_2O (l), H_2O (c)	37.08	38.20	Ligand
6	8.92	7.97	3 H_2O (l)	41.39	40.60	H_2O (c), Ligand

l, lattice; c, coordinated

Table S10. Thermogravimetric analysis for **7-10**.

Compound	1st step loss			2nd Step loss			3rd Step loss		
	Obsd. %	Calcd. %	Loss	Obsd. %	Calcd. %	Loss	Obsd. %	Calcd. %	Loss
7	2.40	2.40	H_2O (l)	15.80	13.40	H_2O (l), 0.5 (4,4′–bpy)	37.30	38.90	0.5 (4,4′–bpy), ligand
8	4.83	4.14	2 H_2O (l)	21.06	18.00	4 H_2O (l), 0.5 (4,4′–bpy)	32.85	37.70	0.5 (4,4′–bpy), ligand
9	4.63	4.35	2 H_2O (l)	25.68	19.72	4,4′–bpy	13.74	13.27	ligand
10	5.15	5.90	3 H_2O (l)	23.90	19.62	H_2O (l), DMF (l), 0.5 (4,4′–bpy)	21.69	20.00	0.5 (4,4′–bpy), ligand

l, lattice